Thermochimica Acta 519 (2011) 90–95

Contents lists available at ScienceDirect

Thermochimica Acta

journal homepage: www.elsevier.com/locate/tca

Effect of low octavinyl-polyhedral oligomeric silsesquioxanes loadings on the melt crystallization and morphology of biodegradable poly(L-lactide)

Jing Yu, Zhaobin Qiu*

State Key laboratory of Chemical Resource Engineering, Key Laboratory of Carbon Fiber and Functional Polymers, Ministry of Education, Beijing University of Chemical Technology, Beijing 100029, China

ARTICLE INFO

Article history:
Received 25 January 2011
Received in revised form 24 February 2011
Accepted 10 March 2011
Available online 21 March 2011

Keywords:
Poly(L-lactide)
Octavinyl-polyhedral oligomeric silsesquioxanes
Nanocomposites
Crystallization behavior
Thermal stability

ABSTRACT

Biodegradable poly(L-lactide) (PLLA)/octavinyl-polyhedral oligomeric silsesquioxanes (ovi-POSS) nanocomposites were prepared via solution and casting method at low loadings of ovi-POSS in this work. Effect of ovi-POSS on the crystallization behavior, spherulitic morphology, crystal structure, and thermal stability of PLLA in the nanocomposites was investigated in detail. It is found that both non-isothermal melt and cold crystallization of PLLA in the nanocomposites are enhanced by the presence of ovi-POSS. In addition, the enhancement becomes more significant with the increase of POSS content to 1 wt%. For isothermal melt crystallization, the overall crystallization rates are faster in the PLLA/ovi-POSS nanocomposites than those in neat PLLA and improved with increasing the ovi-POSS loading; however, the crystallization mechanism and crystal structure of PLLA remain unchanged despite the presence of ovi-POSS. The thermal stability of PLLA in the PLLA/ovi-POSS nanocomposites is reduced slightly relative to neat PLLA.

1. Introduction

Polyhedral oligomeric silsesquioxanes (POSS) are a type of three-dimensional nanofiller and process the structure of cube-octameric frameworks represented by the formula ($R_8Si_8O_{12}$) with an inorganic cube-like core (Si_8O_{12}) surrounded by eight organic corner groups, one or more of which is reactive [1]. The applications of POSS-containing materials have been studied extensively because of the recent commercial availability of many useful precursors. POSS molecules have been introduced into many kinds of polymer matrices via copolymerization and physical blending to prepare higher performance nanostructured organic–inorganic composites in comparison with other inorganic nanofillers [2,3]. Copolymerization is an efficient approach for polymer/POSS nanocomposites, through which the reactive functional groups of POSS may form chemical bonds or chemical link with the monomer, and thus can raise glass transition temperature, enhance mechanical performance and improve thermal stability of polymer [4–7]. However, a majority of polymers, such as linear low-density polyethylene (LLDPE), high-density polyethylene (HDPE), polypropylene (PP), and polystyrene (PS), have been simply blended with POSS to obtain nanocomposites, considering the advantages of low cost and easy industrial implementation [8–11]. It turns out that using this simple blending method, POSS can not only disperse finely but also make great progress on the properties of the polymer matrix.

Poly(L-lactic acid) (PLLA) is an environment-friendly thermoplastic with high strength and high modulus [12], which has been widely used in biomedical, agricultural, and general-purpose plastics fields [12–15], for its excellent biocompatibility and inherent biodegradability. As a semicrystalline polymer, PLLA can crystallize in α-, β-, or γ-forms [16–18], depending on different crystallization conditions. The most common modification, α-form, usually can generate during crystallization from the melt. Recently, a new crystal modification, designated as α′-form, has been discovered and defined as a disordered modification of the α-form [19,20]. It has been reported that the formation of the thermally stable α-form crystals of PLLA, formed at high crystallization temperatures ($T_c > 120\,^\circ C$), is thermodynamically favored, while that of the metastable α′-form crystals is kinetically preferential, formed at low crystallization temperatures ($T_c < 100\,^\circ C$) [19,20]. However, the disadvantages of PLLA, such as poor mechanical properties, slow crystallization rate, and slow degradation rate, have limited the practical applications of PLLA [21,22]. Several methods have been developed to overcome these disadvantages, including copolymer synthesis, polymer blending, and chemical grafting methods [23–25]. A recent trend is to make nanocomposites to improve the properties of PLLA, and this method has been regarded as one of the most effective ways since the nanoparticles can significantly enhance the properties of PLLA even at a very low content. It has

* Corresponding author. Fax: +86 10 64413161.
E-mail addresses: qiuzb@mail.buct.edu.cn, zbqiu99@yahoo.com (Z. Qiu).

0040-6031/$ – see front matter © 2011 Elsevier B.V. All rights reserved.
doi:10.1016/j.tca.2011.03.009

been discovered in the studies on PLLA/carbon nanotube (CNT) nanocomposites that the crystallization of PLLA is accelerated, the hydrolytic degradation of PLLA is enhanced, and the mechanical, electrical, and thermal properties are improved after nanocomposite preparation [26–28]. In addition, there are so many other kinds of nanoparticles, such as layered metal phosphonate, hydroxyapatite, and graphite oxide, which have also been studied on their capability of improving the properties of PLLA [29–31].

In our previous works [32,33], a series of biodegradable PLLA/octaisobutyl-polyhedral oligomeric silsesquioxanes (oib-POSS) nanocomposites were prepared by both solution and casting method and solution and coagulation method at various oib-POSS loading ranging from 1 to 10 wt%. It has been found that no matter through which method the nanocomposites were prepared, the incorporation of oib-POSS has significantly enhanced the crystallization rate, improved mechanical properties and accelerated the hydrolytic degradation of PLLA in the nanocomposites with respect to neat PLLA.

It has also been reported that different functional groups of POSS have different effects on the thermal and morphological properties of polymer matrix [10], due to the different interactions between POSS and polymer matrix. Therefore, in this work, another kind of POSS, octavinyl-polyhedral oligomeric silsesquioxanes (ovi-POSS) was used for preparing the PLLA/ovi-POSS nanocomposites via solution and casting method. The influence of ovi-POSS on the morphology, crystallization behavior, and thermal degradation of PLLA was investigated in detail with various techniques. Moreover, in the previous works [8–11,32,33], the contents of POSS in nanocomposites were usually high in order to better improve the properties of polymer matrix, while the focus of this work is to study the effect of relatively low ovi-POSS loadings on the melt crystallization and morphology of PLLA. It is expected that this research will be helpful for a better understanding of the structure and properties' relationship of biodegradable polymer nanocomposites and for their practical applications.

2. Experimental details

2.1. Materials and preparation of PLLA/ovi-POSS nanocomposites

PLLA ($M_w = 1.69 \times 10^5$ g/mol) was kindly provided by Biomer Company, Germany. Ovi-POSS were purchased from Shenyang Amwest Techology Company, China.

The PLLA/ovi-POSS nanocomposites were prepared through a solution and casting method with chloroform as the mutual solvent. On the one hand, the appropriate amount of ovi-POSS was added into chloroform at a concentration of 1 mg/ml. Then, the mixture was sonicated with a KQ-700DE ultrasonic generator for 2 h to make a uniformly dispersed solution. On the other hand, PLLA was placed into chloroform and stirred for 2 h to dissolve PLLA completely. Next, the ovi-POSS solution was added to the PLLA solution and further stirred for 4 h. The PLLA/ovi-POSS solution was poured into a dish to evaporate the solvent at room temperature for 12 h. The sample was further dried at 80 °C under vacuum for 3 days to remove the solvent completely. Through the aforementioned procedure, PLLA was mixed with the addition of 0.5 and 1 wt% ovi-POSS, respectively. For brevity, they were abbreviated as POSS-0.5 and POSS-1 from now on. For comparison, neat PLLA was stirred for the same time as the nanocomposites.

2.2. Characterizations

Thermal analysis was carried out using a TA instrument differential scanning calorimetry (DSC) Q100 with a Universal Analysis 2000. All operations were performed under nitrogen purge, and the weight of the samples varied between 4 and 6 mg. For nonisothermal melt crystallization, the sample was heated to 190 °C at 20 °C/min, held for 3 min to erase any thermal history, and cooled to 20 °C at 5 °C/min. The crystallization peak temperature was read from the cooling process. For nonisothemal cold crystallization, the sample was heated to 190 °C at 40 °C/min, held for 3 min to erase any thermal history, cooled to 0 °C at 40 °C/min to reach the amorphous state, and then heated to 190 °C again at 20 °C/min. The glass transition temperature, cold crystallization peak temperature, and melting point temperature of neat PLLA and its nanocomposites were read from the second heating traces. For isothermal melt crystallization, the sample was heated to 190 °C at 20 °C/min, held for 3 min to erase any thermal history, cooled to the chosen crystallization temperature at 40 °C/min, and held for a period of time until the isothermal crystallization was complete. The crystallization temperatures chosen in this work were from 120 to 135 °C. The evolution of heat flow with crystallization time was recorded during the isothermal crystallization process for the later data analysis.

An optical microscope (POM) (Olympus BX51) equipped with a temperature controller (Linkam THMS 600) was used to investigate the spherulitic morphology of neat PLLA and the PLLA/ovi-POSS nanocomposites. The samples were first annealed at 190 °C for 3 min and then cooled to 125 °C at 60 °C/min.

Wide angle X-ray diffraction (WAXD) experiments were performed on a Rigaku D/Max 2500 VB2t/PC X-ray diffractometer at room temperature in the range of 5–45° with a scanning rate of 4°/min. The CuKα radiation (λ = 0.15418 nm) source was operated at 40 kV and 200 mA. The samples were first pressed into films with a thickness of around 0.6 mm on a hot stage at 190 °C and then transferred into a vacuum oven at 125 °C for 3 days.

Thermogravimetry analysis (TGA) measurement was performed on a TA Q50 instrument. All operations were performed under nitrogen purge. The sample was heated from room temperature to 580 °C at 20 °C/min.

3. Results and discussion

3.1. Effect of POSS on the nonisothermal crystallization of PLLA in the PLLA/ovi-POSS nanocomposites

It is interesting to study the effect of ovi-POSS on the nonisothermal crystallization behavior of PLLA in the PLLA/ovi-POSS nanocomposites. Nonisothermal melt crystallization of neat PLLA and its nanocomposites was studied by DSC first in this work at 5 °C/min. As shown in Fig. 1, neat PLLA shows a melt crystallization peak temperature (T_{cc}) at around 97.3 °C with a crystallization enthalpy (ΔH_{cc}) being around 3.9 J/g; however, T_{cc}s shift to 98.5 and 112.6 °C with the values of ΔH_{cc} being around 12.6 and 40.3 J/g for POSS-0.5 and POSS-1, respectively. On the basis of the heat of fusion of 100% crystalline (ΔH_m°) PLLA (93 J/g) [34], the degree of crystallinity (W_c) values of neat PLLA and its nanocomposites are determined and normalized with respect to the composition of each component in the composites. The values of W_c are determined to be around 4.2%, 13.6%, and 43.8% for neat PLLA, POSS-0.5 and POSS-1, respectively. It is clear that T_{cc} is significantly increased in the PLLA/ovi-POSS nanocomposites than in neat PLLA; moreover, ΔH_{cc} and W_c are increased in the PLLA/ovi-POSS nanocomposites than in neat PLLA. In addition, the variation of the ovi-POSS loading shows significant influence on the nonisothermal melt crystallization behavior of PLLA in the nanocomposites, since T_{cc} of POSS-1 is about 14 °C higher than that of POSS-0.5, and the values of ΔH_{cc} and W_c of POSS-1 are over 3 times as those of POSS-0.5. The aforementioned results indicate that nonisothermal melt crystallization of PLLA is enhanced by the presence of ovi-POSS in the nanocomposites, and this influence significantly depends on the ovi-POSS loading.

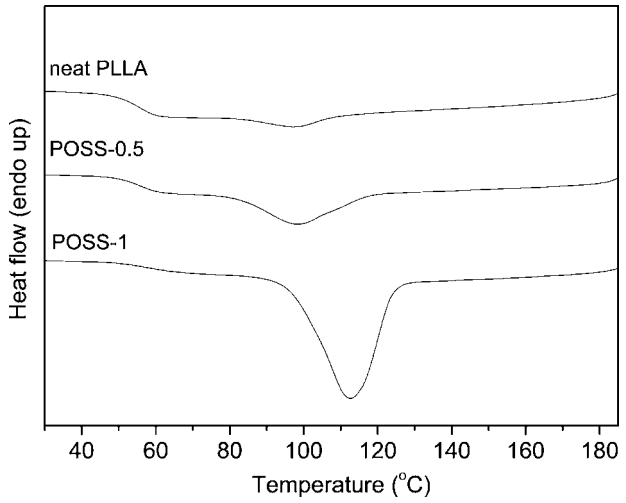

Fig. 1. Nonisothermal melt crystallization of neat PLLA and its nanocomposites at 5 °C/min.

Nonisothermal cold crystallization behavior of neat PLLA and the PLLA/ovi-POSS nanocomposites was further studied with DSC. Fig. 2 shows the DSC heating traces of neat PLLA and its nanocomposites from the amorphous state at 20 °C/min. It is obvious that despite the ovi-POSS loading, the incorporation of ovi-POSS shows little effect on the glass transition temperature (T_g) of PLLA, which is around 61.5 °C. Neat PLLA exhibits a cold crystallization peak temperature (T_{ch}) of 139.2 °C with a cold crystallization enthalpy (ΔH_{ch}) being 7.2 J/g; however, T_{ch}s shift gradually to lower temperature range with increasing the ovi-POSS content in the PLLA/ovi-POSS nanocomposites. For POSS-0.5, T_{ch} shifts to around 136.1 °C, which is only about 3 °C lower than that of neat PLLA, while for POSS-1, T_{ch} shifts to around 116.8 °C, which is about 22 °C lower than that of neat PLLA. Neat PLLA has a melting point (T_m) of 167.1 °C with a heat of fusion (ΔH_m) being 7.4 J/g. In the case of POSS-0.5, T_m is almost the same as neat PLLA, however, ΔH_m is 18.3 J/g, which is more than two times as that of neat PLLA. In the case of POSS-1, T_m is nearly 3 °C lower than that of neat PLLA, and ΔH_m is 40.9 J/g, over 5 times higher than that of neat PLLA. It is also found that W_c is around 8.0% for neat PLLA, increasing to be 19.8% for POSS-0.5 and 44.4% for POSS-1. It is apparent that the presence of ovi-POSS enhances nonisothermal cold crystallization of PLLA significantly in the nanocomposites relative to neat PLLA, especially when the POSS content increases to 1 wt%. All of the above mentioned parameters are summarized in Table 1 for comparison. It can thus be concluded that compared to neat PLLA, both nonisothermal melt and cold crystallization of PLLA are enhanced significantly in the PLLA/ovi-POSS nanocomposites, indicating that ovi-POSS may play a role of nucleating agent during the nonisothermal melt and cold crystallization of PLLA.

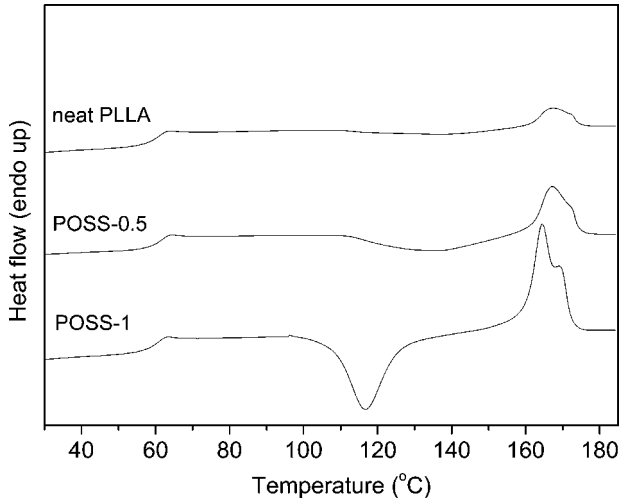

Fig. 2. DSC heating traces of neat PLLA and its nanocomposites at 20 °C/min from the amorphous state.

Table 1
Summary of some characteristic parameters for neat PLLA and its nanocomposites during nonisothermal cold crystallization at 20 °C/min.

Samples	T_g (°C)	T_{ch} (°C)	ΔH_{ch} (J/g)	T_m (°C)	ΔH_m (J/g)	W_c (%)
Neat PLLA	61.3	139.2	7.2	167.1	7.4	8.0
POSS-0.5	62.1	136.1	18.2	167.3	18.3	19.8
POSS-1	61.0	116.8	40.9	164.5	40.9	44.4

3.2. *Effect of POSS on the isothermal melt crystallization of PLLA in the PLLA/ovi-POSS nanocomposites*

Nonisothermal melt and cold crystallization of neat PLLA and the PLLA/ovi-POSS nanocomposites were studied with DSC in the above section. In this section, the influence of ovi-POSS on the isothermal melt crystallization of PLLA in the PLLA/ovi-POSS nanocomposites was further investigated with DSC. As introduced in Section 2, the overall isothermal melt crystallization kinetics of neat PLLA and its nanocomposites were studied with DSC in a temperature range from 120 to 135 °C. Fig. 3 shows the plots of relative degree of crystallinity against crystallization time for all the samples. On one hand, it is clear from Fig. 3 that all these curves have the similar sigmoid shape, and the corresponding crystallization time for all the samples becomes longer with increasing the crystallization temperature. On the other hand, the corresponding crystallization time for the PLLA/ovi-POSS nanocomposites becomes shorter with increasing the ovi-POSS loading at the same crystallization temperature. For instance, it took neat PLLA almost 36 min to finish crystallization at 125 °C, but for the POSS-0.5 and POSS-1 samples, the time required to finish crystallization became only around 25 and 5 min, respectively. It is obvious that the incorporation of ovi-POSS enhances the isothermal melt crystallization of PLLA remarkably when compared with neat PLLA; moreover, with increasing the ovi-POSS content, the isothermal crystallization of PLLA becomes faster.

The well-known Avrami equation is often used to analyze the isothermal crystallization kinetics of polymers [35,36]; it assumes that the relative degree of crystallinity develops with crystallization time as

$$1 - X_t = \exp(-kt^n) \quad (1)$$

where X_t is the relative degree of crystallinity at crystallization time (t), n is the Avrami exponent depending on the nature of nucleation and growth geometry of the crystals, and k is the crystallization rate constant involving both nucleation and growth rate parameters. In the case of the DSC experiment, X_t at t is defined as the ratio of the area under the exothermic curve between the onset crystallization time and t to the whole area under the exothermic curve from the onset crystallization time to the end crystallization time. Fig. 4 shows the Avrami plots of neat PLLA and its nanocomposites, from which the Avrami parameters n and k can be obtained from the slopes and the interceptions, respectively.

The Avrami parameters are summarized in Table 2 for neat PLLA and its nanocomposites crystallized at different crystallization temperatures (T_cs). It can be found that the average values of n are around 2.3 and almost unchanged with the addition of ovi-POSS, suggesting that the incorporation of ovi-POSS may not change the

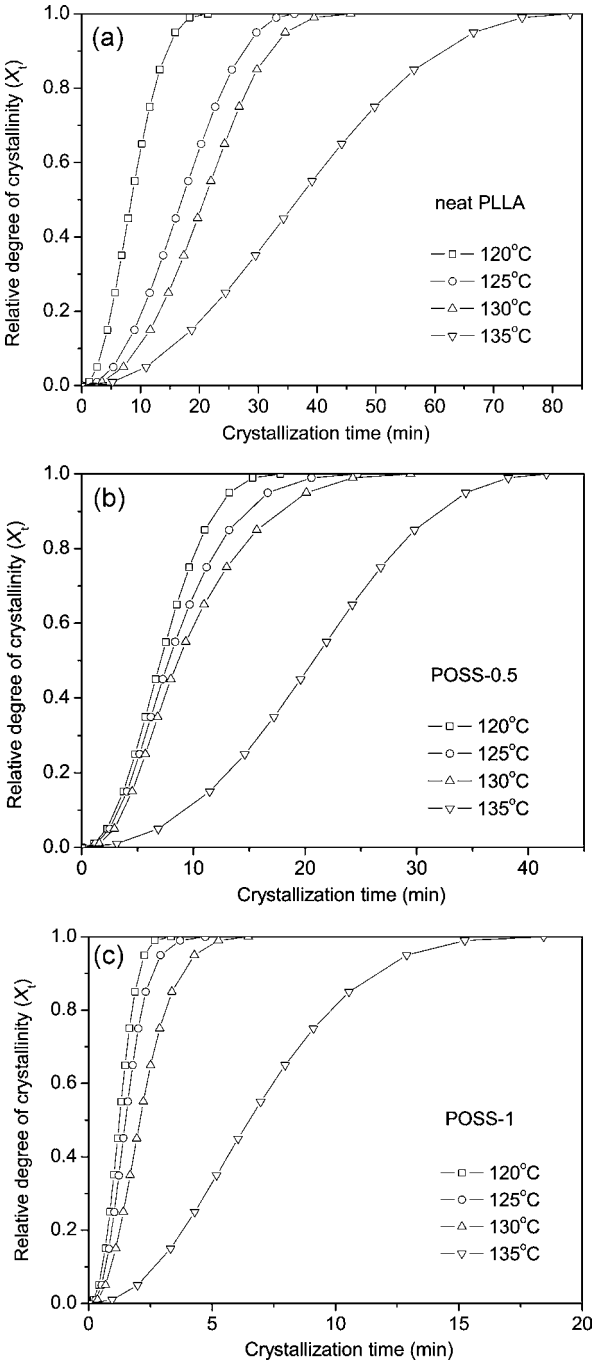

Fig. 3. Variation of relative degree of crystallinity with crystallization time at different T_cs for (a) neat PLLA, (b) POSS-0.5, and (c) POSS-1.

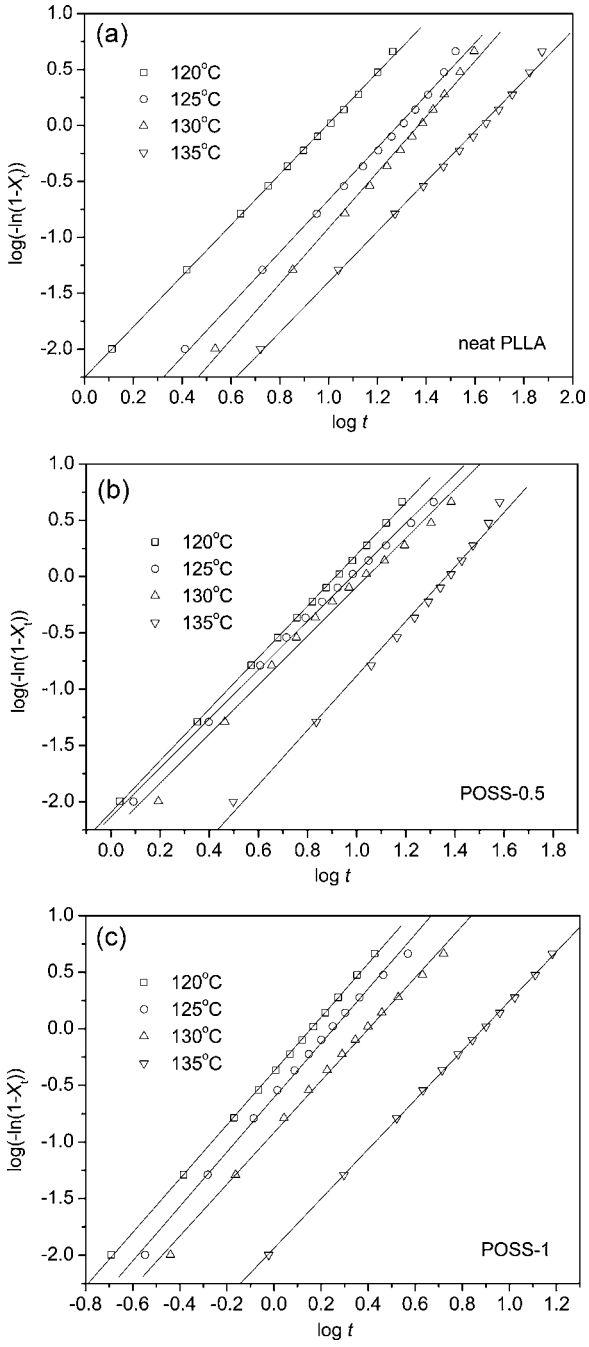

Fig. 4. The related Avrami plots for (a) neat PLLA, (b) POSS-0.5, and (c) POSS-1.

Table 2
Summary of isothermal crystallization kinetics parameters of neat PLLA and its nanocomposites at different T_cs based on the Avrami equation.

Samples	T_c (°C)	n	k (min^{-n})	$t_{0.5}$ (min)	$1/t_{0.5}$ (min^{-1})
Neat PLLA	120	2.3	5.57×10^{-3}	8.35	1.20×10^{-1}
	125	2.3	9.85×10^{-4}	16.45	6.08×10^{-2}
	130	2.5	3.90×10^{-4}	20.15	4.96×10^{-2}
	135	2.2	2.26×10^{-4}	35.61	2.81×10^{-2}
POSS-0.5	120	2.3	8.05×10^{-3}	7.00	1.43×10^{-1}
	125	2.2	7.34×10^{-3}	8.11	1.23×10^{-1}
	130	2.2	5.36×10^{-3}	9.34	1.07×10^{-1}
	135	2.4	4.99×10^{-4}	19.88	5.03×10^{-2}
POSS-1	120	2.4	4.23×10^{-1}	1.23	8.12×10^{-1}
	125	2.4	2.47×10^{-1}	1.54	6.51×10^{-1}
	130	2.3	1.21×10^{-1}	2.15	4.66×10^{-1}
	135	2.2	1.15×10^{-2}	6.53	1.53×10^{-1}

crystallization mechanism of PLLA in the PLLA/ovi-POSS nanocomposites. The k values are also listed in Table 2. However, it should be noted that it is difficult to compare the overall crystallization rate directly from the k values because the unit of k is min^{-n} and n is not constant. Thus, the crystallization half-time ($t_{0.5}$), the time required to achieve 50% of the final crystallinity of the samples, is introduced for discussing crystallization kinetics. The crystallization rate can thus be easily described by the reciprocal of $t_{0.5}$. The value of $t_{0.5}$ is calculated by the following equation:

$$t_{0.5} = \left(\frac{\ln 2}{k}\right)^{1/n} \quad (2)$$

The values of $t_{0.5}$ and $1/t_{0.5}$ of neat PLLA and its nanocomposites are listed in Table 2 as well, from which the effects of T_c and the ovi-POSS loading on the variation of overall crystallization rate

can be obtained obviously. As shown in Table 2, the values of $t_{0.5}$ increase with increasing T_c for both neat PLLA and its nanocomposites, indicating that the overall isothermal crystallization rate decreases with the increase of T_c. Such results are reasonable since it is difficult for the samples to nucleate at high T_c, thereby resulting in the reduction of the overall crystallization rate. In addition, the $t_{0.5}$ values are smaller in the nanocomposites than in neat PLLA at a given T_c, indicating again that the isothermal melt crystallization of PLLA is accelerated by the presence of ovi-POSS. Such results suggest that ovi-POSS may play a significant role as nucleating agent during the isothermal melt crystallization of PLLA in the PLLA/ovi-POSS nanocomposites. Moreover, the $1/t_{0.5}$ values, representing the isothermal melt crystallization rate, are also shown in Table 2. The values of $1/t_{0.5}$ increase with increasing the ovi-POSS loading in the PLLA/ovi-POSS nanocomposites at a given T_c, suggesting that the ovi-POSS loading has a significant effect on the crystallization of PLLA. Similar results have also been found in PP/SiO_2 nanocomposites [37]. In sum, the overall isothermal melt crystallization of PLLA is accelerated by the presence of ovi-POSS in the PLLA/ovi-POSS nanocomposites relative to neat PLLA; moreover, the enhancement of the overall crystallization rate of PLLA is influenced by the ovi-POSS loading. The DSC results reported herein are consistent with the spherulitic morphology study in the following section.

3.3. *Effect of POSS on the spherulitic morphology and crystal structure of PLLA in the PLLA/ovi-POSS nanocomposites*

Fig. 5 displays the spherulitic morphology of neat PLLA and its nanocomposites crystallized at 125 °C. As shown in Fig. 5a, the well-developed spherulites of neat PLLA grew to a size of about 150 μm in diameter, and the boundaries are clear. Parts b and c of Fig. 5 illustrate the POM images of the nanocomposites with the ovi-POSS loadings of 0.5 and 1 wt%, respectively. It is clear that the size of PLLA spherulites in the PLLA/ovi-POSS nanocomposites is much smaller than that in neat PLLA, and correspondingly, the number of PLLA spherulites is greater in the PLLA/ovi-POSS nanocomposites than in neat PLLA. In addition, the PLLA spherulite boundaries become much obscurer in the PLLA/ovi-POSS nanocomposites, especially when the ovi-POSS content increases to 1 wt%. Such variations indicate that the nucleation density of PLLA spherulites increases dramatically in the PLLA/ovi-POSS nanocomposites because of the nucleating agent effect of ovi-POSS. In brief, the presence of ovi-POSS and their contents in the PLLA matrix are the main factors, which influence the spherulitic morphology and the overall crystallization process of PLLA significantly.

It is also essential to study the effect of ovi-POSS on the crystal structure of PLLA in the PLLA/ovi-POSS nanocomposites. As introduced in Section 2, WAXD experiments were performed to investigate the crystal structures of neat PLLA and its nanocomposites, all crystallized at 125 °C in α-form. In Fig. 6, the presence of many strong diffraction peaks illustrates that ovi-POSS are highly crystalline. Moreover, the characteristic diffraction peak of ovi-POSS at around 9.7° [11] also appears in the PLLA/ovi-POSS nanocomposites, indicating that ovi-POSS may exist as separate crystals, or ovi-POSS particles are able to crystallize when they are dispersed in the PLLA matrix. Similar results are also found in the PLLA/oib-POSS nanocomposites in our previous work [32,33]. For neat PLLA, two sharp characteristic diffraction peaks are shown at 16.25° and 18.57°, corresponding to (2 0 0)/(1 1 0) and (2 0 3) planes, respectively [38]. For the PLLA/ovi-POSS nanocomposites, the similar diffraction patterns are also observed in Fig. 6, which indicates incorporating with ovi-POSS does not modify the crystal structure of PLLA. In short, the crystal structure of PLLA remains unchanged despite the addition of ovi-POSS in the PLLA/ovi-POSS nanocomposites. It should also be noted that the dispersion of ovi-POSS in the PLLA matrix has not been checked in this study. It is clear that the crystallization and morphology of PLLA must be influenced by the dispersion of ovi-POSS. The investigation of the ovi-POSS dispersion is still under way and will be reported in the forthcoming research.

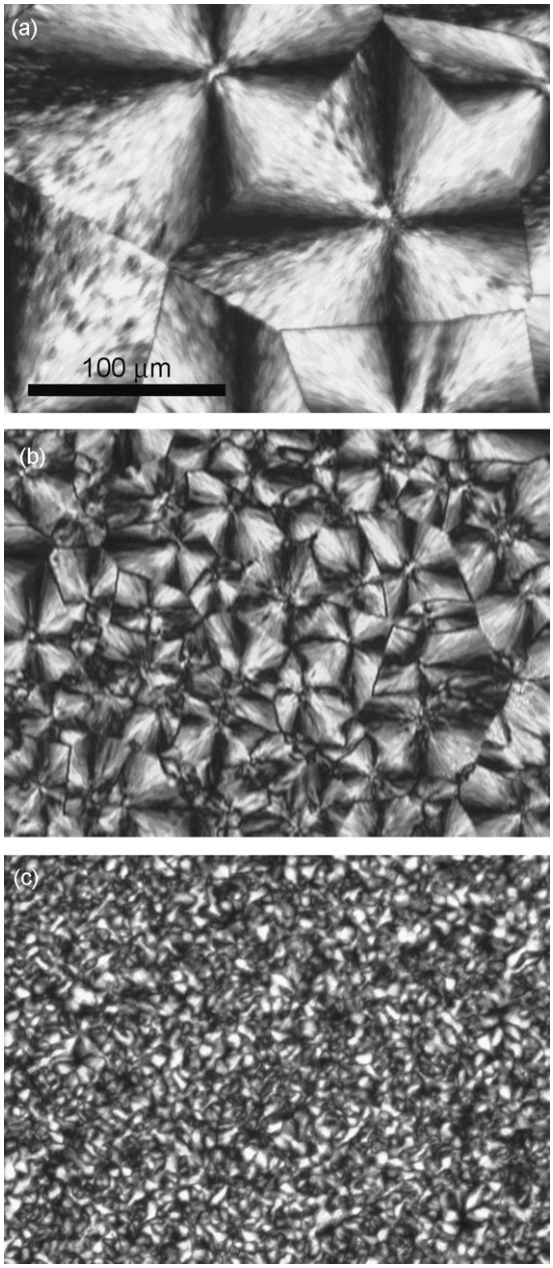

Fig. 5. POM images of neat PLLA and its nanocomposites crystallized at 125 °C; (a) neat PLLA, (b) POSS-0.5, and (c) POSS-1.

3.4. *Effect of POSS on the thermal stability of PLLA in the PLLA/ovi-POSS nanocomposites*

The effect of ovi-POSS on the thermal stability of PLLA was also investigated in this work. Fig. 7 shows the TGA curves of neat PLLA and its nanocomposites. It is apparent that both neat PLLA and its nanocomposites present a similar degradation profile, which suggests the addition of ovi-POSS does not change the degradation mechanism of the PLLA matrix. The degradation temperature at 5% weight loss (T_d) of neat PLLA is 337.4 °C, while T_d of neat ovi-POSS is 218.2 °C, as shown in Fig. 7. For the PLLA/ovi-POSS nanocomposites, T_ds are 332.9 and 331.8 °C for POSS-0.5 and POSS-1, respectively,

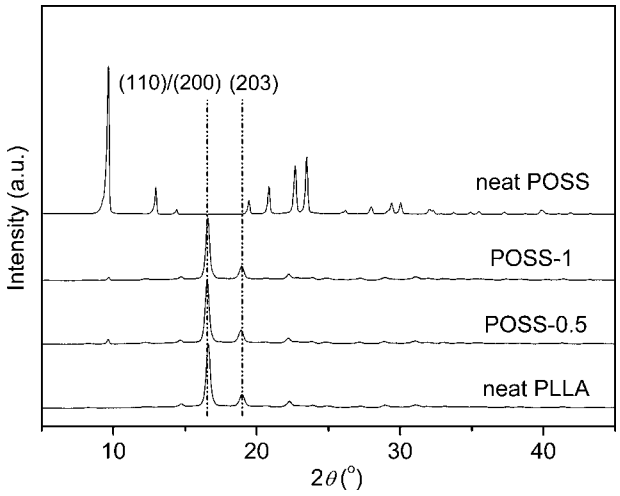

Fig. 6. WAXD patterns of neat PLLA and its nanocomposites.

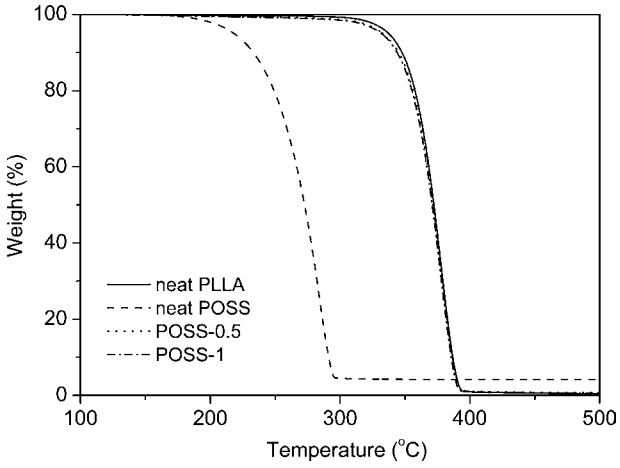

Fig. 7. TGA curves of neat ovi-POSS, neat PLLA, and their nanocomposites.

demonstrating that the thermal stability of the PLLA matrix is reduced slightly by the ovi-POSS adding. The slightly reduced thermal stability indicates that there are no strong interactions between ovi-POSS and the PLLA matrix [10].

4. Conclusions

Biodegradable PLLA/ovi-POSS nanocomposites were successfully prepared in this work via solution and casting method at low ovi-POSS loadings. Effect of low loadings of ovi-POSS on the nonisothermal melt and cold crystallization behavior, isothermal melt crystallization kinetics, spherulitic morphology, crystal structure, and thermal stability of PLLA in the PLLA/ovi-POSS nanocomposites was investigated in detail with DSC, POM, WAXD, and TGA, and compared with those of neat PLLA. It is found that the presence of ovi-POSS enhances both nonisothermal melt and cold crystallization behavior of PLLA in the nanocomposites apparently relative to neat PLLA. Isothermal melt crystallization kinetics of neat PLLA and its nanocomposites was studied with DSC at various crystallization temperatures and analyzed by the Avrami equation. The overall crystallization rates are faster in the PLLA/ovi-POSS nanocomposites than in neat PLLA; however, the crystallization mechanism of PLLA remains unchanged despite the addition of ovi-POSS. The POM results show that the number of PLLA spherulites is greater in the PLLA/ovi-POSS nanocomposites than in neat PLLA; moreover, the size of PLLA spherulites is smaller in the PLLA/ovi-POSS nanocomposites than in neat PLLA. The increased nucleation density of PLLA spherulites in the nanocomposites indicates that ovi-POSS act as an effective nucleating agent during the isothermal crystallization process of PLLA. Based on the WAXD study, it can be confirmed that the incorporation of ovi-POSS does not modify the crystal structure of PLLA in the nanocomposites relative to neat PLLA. In addition, the thermal stability of PLLA matrix is reduced slightly with the incorporation of ovi-POSS in the PLLA/ovi-POSS nanocomposites, which indicates interaction between ovi-POSS and the PLLA matrix is not strong.

Acknowledgements

Part of this work is financially supported by the National Natural Science Foundation, China (20974012) and the Fundamental Research Funds for the Central Universities (ZZ1005).

References

[1] D.B. Cordes, P.D. Lickiss, F. Rataboul, Chem. Rev. 110 (2010) 2081–2173.
[2] A. Fina, O. Monticelli, G. Camino, J. Mater. Chem. 20 (2010) 9297–9305.
[3] J. Wu, P.T. Mather, Polym. Rev. 49 (2009) 25–63.
[4] Y. Liu, X. Yang, W. Zhang, S. Zheng, Polymer 47 (2006) 6814–6825.
[5] Y. Ni, S. Zheng, J. Polym. Sci. B: Polym. Phys. 45 (2007) 2201–2214.
[6] K. Zeng, S. Zheng, Macromol. Chem. Phys. 210 (2009) 783–791.
[7] B. Kim, P. Mather, Macromolecules 39 (2006) 9253–9260.
[8] M.J. Hato, S.S. Ray, A.S. Luyt, Macromol. Mater. Eng. 293 (2008) 752–762.
[9] M. Joshi, B.S. Butola, G. Simon, N. Kukaleva, Macromolecules 39 (2006) 1839–1849.
[10] A. Fina, D. Tabuani, A. Frache, G. Camino, Polymer 46 (2005) 7855–7866.
[11] Y. Feng, Y. Jia, S. Guang, H. Xu, J. Appl. Polym. Sci. 115 (2010) 2212–2220.
[12] D. Garlotta, J. Polym. Environ. 9 (2001) 63–84.
[13] J. Bogaert, P. Coszac, Macromol. Symp. 153 (2000) 287–303.
[14] R. Drumright, P. Gruber, D. Henton, Adv. Mater. 12 (2000) 1841–1846.
[15] Y. Ikada, H. Tsuji, Macromol. Rapid Commun. 21 (2000) 117–132.
[16] P. De Sabtus, J. Kovacs, Biopolymers 6 (1968) 299–306.
[17] B. Eling, S. Gogolewski, A.J. Pennings, Polymer 23 (1982) 1587–1593.
[18] L. Cartier, T. Okihara, Y. Ikada, H. Tsuji, J. Puiggali, B. Lotz, Polymer 41 (2000) 8909–8919.
[19] P. Pan, W. Kai, B. Zhu, T. Dong, Y. Inoue, Macromolecules 40 (2007) 6898–6905.
[20] P. Pan, Z. Liang, B. Zhu, T. Dong, Y. Inoue, Macromolecules 42 (2009) 3374–3380.
[21] M. Di Lorenzo, Eur. Polym. J. 41 (2005) 569–575.
[22] J. Lu, Z. Qiu, W. Yang, Polymer 48 (2007) 4196–4204.
[23] J. Chang, Y. An, G. Sur, J. Polym. Sci. B: Polym. Phys. 41 (2003) 94–103.
[24] N. Fukuda, H. Tsuji, J. Appl. Polym. Sci. 96 (2005) 190–199.
[25] T. Thostenson, Z. Ren, T. Chou, Compos. Sci. Technol. 61 (2001) 1899–1912.
[26] Y. Zhao, Z. Qiu, W. Yang, J. Phys. Chem. B 112 (2008) 16461–16468.
[27] D. Zhang, M. Kandadai, J. Cech, S. Roth, S. Curran, J. Phys. Chem. B 110 (2006) 12910–12915.
[28] S. Kim, B. Park, J. Yoon, H. Jin, Eur. Polym. J. 43 (2007) 1729–1735.
[29] P. Pan, Z. Liang, A. Cao, Y. Inoue, ACS Appl. Mater. Interfaces 1 (2009) 402–411.
[30] C. Delabarde, C. Plummer, P. Bourban, J. Manson, Compos. Sci. Technol. 70 (2010) 1813–1819.
[31] H. Lei, W. Kai, J. Yang, Y. Inoue, Polym. Degrad. Stab. 95 (2010) 2619–2627.
[32] Z. Qiu, H. Pan, Compos. Sci. Technol. 70 (2010) 1089–1094.
[33] H. Pan, Z. Qiu, Macromolecules 43 (2010) 1499–1506.
[34] E. Fischer, H. Sterzel, G. Wegner, Kolloid Z. Z. Polym. 251 (1973) 980–990.
[35] M. Avrami, J. Chem. Phys. 8 (1940) 212–224.
[36] M. Avrami, J. Chem. Phys. 9 (1941) 177–184.
[37] G.Z. Papageorgiou, D.S. Achilias, D.N. Bikiaris, G.P. Karayannidis, Thermochim. Acta 427 (2005) 117–128.
[38] W. Hoogsteen, A. Postema, A. Pennings, G. Ten Brinke, P. Zugenmaier, Macromolecules 23 (1990) 634–642.